Velocity difference statistics in turbulence

Sunghwan Jung* and Harry L. Swinney

Center for Nonlinear Dynamics and Department of Physics, The University of Texas at Austin, Austin, Texas 78712, USA
(Received 14 February 2005; published 24 August 2005)

We unify two approaches that have been taken to explain the non-Gaussian probability distribution functions (PDFs) obtained in measurements of longitudinal velocity differences in turbulence, and we apply our approach to Couette-Taylor turbulence data. The first approach we consider was developed by Castaing and co-workers, who obtained the non-Gaussian velocity difference PDF from a superposition of Gaussian distributions for subsystems that have a particular energy dissipation rate at a fixed length scale [Castaing *et al.*, Physica D **46**, 177 (1990)]. Another approach was proposed by Beck and Cohen, who showed that the observed PDFs can be obtained from a superposition of Gaussian velocity difference PDFs in subsystems conditioned on the value of an intensive variable (inverse "effective temperature") in each subsystem [Beck and Cohen, Physica A **322**, 267 (2003)]. The intensive variable was defined for subsystems assuming local thermodynamic equilibrium, but no method was proposed for determining the size of a subsystem. We show that the Castaing and Beck-Cohen methods are related, and we present a way to determine subsystem size in the Beck-Cohen method. The application of our approach to Couette-Taylor turbulence (Reynolds number 540 000) yields a log-normal distribution of the intensive parameter, and the resultant velocity difference PDF agrees well the observed non-Gaussian velocity difference PDFs.

I. INTRODUCTION

In Kolmogorov's 1941 theory (K41), the energy in fully developed three-dimensional turbulence cascades from large scales to small scales where it is dissipated [1]. Turbulence in the cascade (the inertial range) is characterized by the probability distribution function (PDF) $P(\delta v_r)$ for longitudinal velocity differences over a distance r, $\delta v_r(x) = \hat{e}_r \cdot [\vec{v}(x+r) - \vec{v}(x)]$, where $\hat{e}_r$ is the direction of separation [2]. For r approaching the integral scale where energy is injected, the PDF is Gaussian, while in the inertial range extending down to the dissipation scale η, intermittent large fluctuations lead to a non-Gaussian PDF with approximately exponential tails [3].

Kolmogorov assumed a constant energy dissipation rate per unit volume, ε [1]. In 1944 Landau [4] suggested that fluctuations of ε averaged at scale r, $\varepsilon_r(\vec{x}, t)$ $\times (= \int_{\vec{x}}^{\vec{x}+\vec{r}} \varepsilon(\vec{x}', t) d\vec{x}')$ play a key role in turbulence. Such fluctuations were subsequently observed in many experiments [5–7]. In 1962 Kolmogorov [8] and Obukhov [9] proposed a log-normal distribution of ε_r in the inertial range. The log-normal distribution was obtained in subsequent experiments and numerical simulations ε_r [10–13]. The non-Gaussian PDF of δv_r and the log-normal PDF of ε_r characterize turbulent flows.

Different approaches have been taken by Castaing *et al.* [14] and by Beck and Cohen [15] to understand the non-Gaussian $P(\delta v_r)$. Castaing *et al.* assumed at subsystems have different values of ε_r, but the subsystems have Gaussian PDFs of δv_r; this assumption is supported by experiments.

Beck and Cohen took a statistical mechanics approach, assuming that subsystems have a well-defined "effective

temperature," which for turbulent flow is identified with the variance of δv_r. The resultant $P(\delta v_r)$ depends on the statistics of the distribution for the inverse effective temperatures in the subsystems. This dependence of the statistical distribution $P(\delta v_r)$ on the statistical distribution of subsystems led Beck and Cohen to call their approach *superstatistics* [15].

In this paper we note that the approaches of Castaing *et al.* and Beck and Cohen are both based on Bayes' theorem,

$$P(x) = \int P(x|y)P(y)dy, \tag{1}$$

which is used to obtain the non-Gaussian $P(\delta v_r)$ from a conditional mixing of Gaussian PDFs in subsystems. However, the subsystems are chosen differently in the two approaches.

We propose a method that does not require a determination of ε_r from experimental data, nor does it require a fitting parameter to obtain the effective temperature PDF. We show that subsystems with Gaussian statistics can be chosen by examining moments of velocity difference distributions in the subsystems. Our method, which involves no fitting parameters, leads to predictions for the non-Gaussian $P(\delta v_r)$ that are in accord with data for turbulent Couette-Taylor flow [16].

In Sec. II we present the Castaing *et al.* and Beck and Cohen methods, and in Sec. III we describe the Couette-Taylor experiments and present results for $P(\delta v_r)$. Section IV shows how subsystems can be systematically chosen to obtain a prediction for $P(\delta v_r)$. The conclusions are presented in Sec. V.

II. THEORY

A. Method of Castaing *et al.*

Castaing *et al.* [14] started with the observation from their experiments that velocity difference distributions for a given

---

*Electronic address: sunnyjsh@chaos.utexas.edu

ε_r are Gaussian, and that ε_r is described by a log-normal distribution [14,17–21]. The log-normal distribution for ε_r has also been obtained for ε_r in other experiments on fully developed turbulence [18,22–24], and in analyses of images of cloud patterns [25], effective temperature fields in turbulence [26], and magnetic fields in solar winds [27].

To describe the evolution of $P(\delta v_r)$ from Gaussian at large scales to non-Gaussian at small scales [28–30], Castaing *et al.* proposed [14,17]

$$P(\delta v_r) = \int P(\varepsilon_r) P(\delta v_r | \varepsilon_r) d\varepsilon_r. \tag{2}$$

The conditional PDF $P(\delta v_r | \varepsilon_r)$ in Eq. (2) is assumed to be a Gaussian distribution, $P(\delta v_r | \varepsilon_r) = e^{-(\delta v_r)^2/(r\varepsilon_r)^{2/3}}$, in accord with experimental observations [31–33]. Kolmogorov [8], Obukhov [9], and Castaing [14] assumed a log-normal distribution of ε_r,

$$P(\varepsilon_r) = \frac{1}{\lambda_\varepsilon (2\pi)^{1/2} \varepsilon_r} \exp\left(-\frac{(\ln \varepsilon_r - m_\varepsilon)^2}{2\lambda_\varepsilon^2}\right), \tag{3}$$

where m_ε and λ_ε are, respectively, the mean and the standard deviation of $\ln \varepsilon_r$.

A difficulty in applying the approach of Castaing *et al.* is that energy dissipation rate at length scale r, ε_r, is not directly measured in experiments. By assuming homogeneous and isotropic conditions, $\varepsilon_r(x)$ is defined as $15\nu \int_x^{x+r} (\partial v/\partial x)^2 dx$. In practice, ε_r is determined from time series data,

$$\varepsilon_r = \frac{15\nu}{(\Delta x)^2} \sum_{i=1}^{N-1} [v(x_{i+1}) - v(x_i)]^2, \tag{4}$$

where $\Delta x (\equiv x_2 - x_1)$ is the sampling separation the summation i is over subsystems and $x_N - x_1 = r$ [33–35]. Even with this assumption, determination of $\varepsilon_r(x)$ is difficult because of errors in evaluating the derivative from velocity data. Further error arises from the application of the Taylor frozen hypothesis at high frequencies [24,36–44].

B. Superstatistics of Beck and Cohen

Beck and Cohen's statistical approach considers a system far from thermodynamic equilibrium to consist of subsystems in local thermodynamic equilibrium [15]. Each subsystem has a well-defined "effective temperature," but the subsystem effective temperatures need not be the same since the whole system is not in equilibrium. Beck and Cohen identify $(\delta v_r)^2$ with the kinetic energy of eddies of size r, $E(\delta v_r) = \frac{1}{2}(\delta v_r)^2$, and the variance of δv_r is identified with an inverse effective temperature β [45], given for a subsystem of size d by

$$\beta_d = \frac{1}{\langle (\delta v_r)^2 \rangle_d - (\langle \delta v_r \rangle_d)^2}, \tag{5}$$

where $\langle \cdot \rangle_d$ is an average over the size d. Then we have
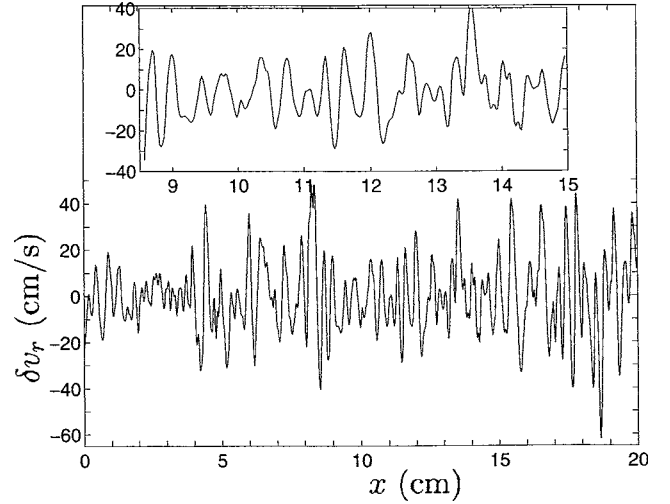

FIG. 1. An example of the Couette-Taylor velocity difference data, obtained by subtracting velocities at two points with a separation $r = 46\eta = 0.134$ cm, where η is the Kolmogorov length scale. The inset shows the velocity differences on a finer length scale.

$$P(\delta v_r) = \int_0^\infty P(\beta_d) P(\delta v_r | \beta_d) d\beta_d. \tag{6}$$

where $P(\beta_d)$ is the distribution of inverse effective temperature in subsystems of size d.

A particular choice of $P(\beta_d)$, the χ^2 distribution, leads to the distribution associated with the nonextensive statistical mechanics of Tsallis, $P(E) = [1 + \beta(q-1)E]^{-1/(q-1)}$, where q is a parameter characterizing the nonextensivity $[S(1+2) = S(1) + S(2) + (1-q)S(1)S(2)$, where S is entropy function] [15,46]. A phenomenology similar to Beck and Cohen's was used in earlier oceanographic analysis that described the global non-Gaussian distribution of ocean surface velocity as a mixture of local Gaussians with χ^2-distributed variance [47,48]. The method of Beck and Cohen has been applied to fully developed turbulence [49,50] by introducing a fitting parameter to determine the PDF of inverse effective temperature, rather than by directly measuring the PDF of inverse effective temperature.

The Beck-Cohen method requires that the size d should be large compared to the distance r separating two points, and d should also be large enough so the subsystems contain enough data points to yield good statistics, but d must also be small enough so that subsystems are each described by a Gaussian distribution. Beck determined the size of d using a fitting parameter involving the kurtosis of $P(\delta v_r)$ [50].

C. Unified view of PDFs

The Castaing and Beck-Cohen methods are similar except in the way they divide a system into subsystems. Castaing *et al.* sample velocity differences conditioned by the averaged energy dissipation rate ε_r, while Beck and Cohen use velocity differences conditioned by the inverse effective temperature β_d. Castaing *et al.* need one fixed length scale, the separation distance r between two points; δv_r and ε_r are defined at this scale and are related through Bayes' theorem. The
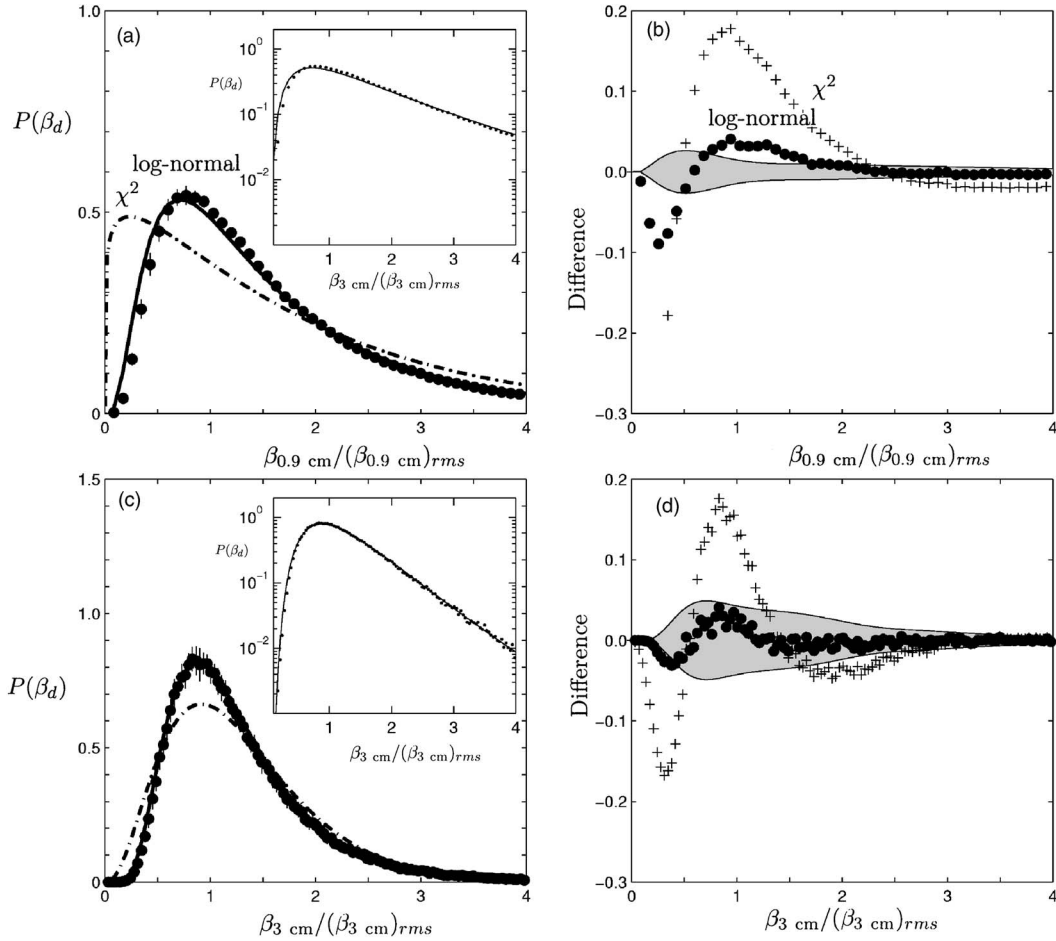
FIG. 2. Comparison of χ^2 and log-normal distributions to the experimental distribution for inverse effective temperature in subsystems of size (a) $d=0.9$ cm and (c) $d=3$ cm. The dashed-dotted lines represent the χ^2 distribution, and the solid line represents the log-normal distribution; both have the same mean and variance as the 20 independent experiments (error bars correspond to one standard deviation). The panels on the right, (b) and (d), show the difference between the experimental PDF for β_d and the χ^2 (plus signs) and log-normal (bullets) distributions for (a) $d=0.9$ cm and (c) $d=3$ cm. The shaded area represents the experimental uncertainty (standard deviation of 20 experiments).

Beck-Cohen method involves two length scales, the distance r separating two points and the size d of the subsystems in the statistical analysis.

The Castaing and Beck-Cohen methods can be connected if the two conditioning variables (ε_r and β_d) are correlated. Using Eq. (2) and Bayes' theorem, we convert Castaing's method into Beck-Cohen's method,

$$P(\delta v_r) = \int_0^\infty P(\delta v_r|\varepsilon_r)P(\varepsilon_r)d\varepsilon_r$$

$$= \int_0^\infty \int_0^\infty P(\delta v_r|\beta_d)P(\beta_d|\varepsilon_r)d\beta_d P(\varepsilon_r)d\varepsilon_r$$

$$= \int_0^\infty P(\delta v_r|\beta_d)\left[\int_0^\infty P(\beta_d|\varepsilon_r)P(\varepsilon_r)d\varepsilon_r\right]d\beta_d \quad (7)$$

$$= \int_0^\infty P(\delta v_r|\beta_d)P(\beta_d)d\beta_d. \quad (8)$$

Now, let us assume a log-normal distribution of β_d at the fixed ε_r,

$$P(\beta_d|\varepsilon_r) \propto \frac{1}{\beta_d} \exp\left[-\frac{(\ln \beta_d - a \ln \varepsilon_r)^2}{2\lambda_t^2}\right], \quad (9)$$

where λ_t is the standard deviation of $\ln \beta_d$ conditioned to ε_r, and a is a parameter. Using Eqs. (3), (7), and (9), we have

$$P(\delta v_r) \propto \int_0^\infty P(\delta v_r|\beta_d)\int_0^\infty \exp\left(-\frac{(\ln \beta_d - a \ln \varepsilon_r)^2}{2\lambda_t^2}\right)$$

$$\times\exp\left(-\frac{(\ln \varepsilon_r - m_\varepsilon)^2}{2\lambda_\varepsilon^2}\right)d(\ln \varepsilon_r)d(\ln \beta_d)$$

$$\propto \int_0^\infty P(\delta v_r|\beta_d)\exp\left(-\frac{(\ln \beta_d - m)^2}{\lambda_\varepsilon^2\lambda_t^2}\right)d(\ln \beta_d).$$

$$(10)$$

Thus with the assumption of a log-normal distribution of β_d conditioned on ε_r, we have that Castaing's method is equivalent to Beck-Cohen's method. In Sec. IV D, the log-normal PDF of $P(\beta_d|\varepsilon_r)$ is verified in experiments.
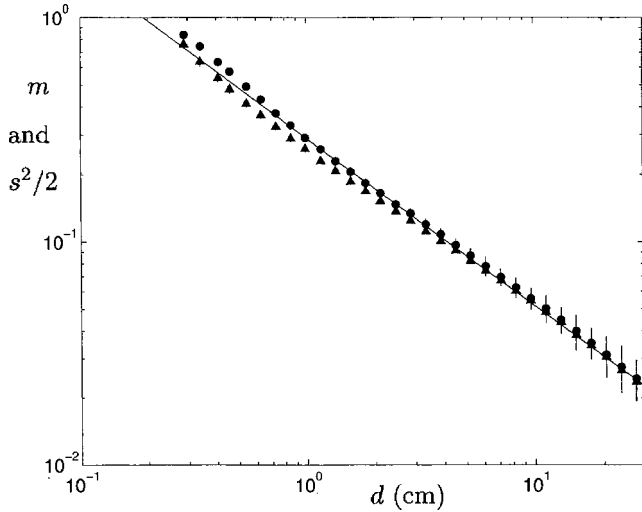
FIG. 3. The parameters $s^2/2$ (circles) and m (triangles), obtained from fits of the inverse effective temperature β_d (deduced from Couette-Taylor turbulence data) to a log-normal distribution, as a function of subsystem size d [see Eq. (11)]. (s and m are the variance and mean of logarithmic inverse effective temperature.) The parameters $s^2/2$ and m are approximately equal (see text) and are described by a power law, $m \propto d^{-3/4}$ (solid line).
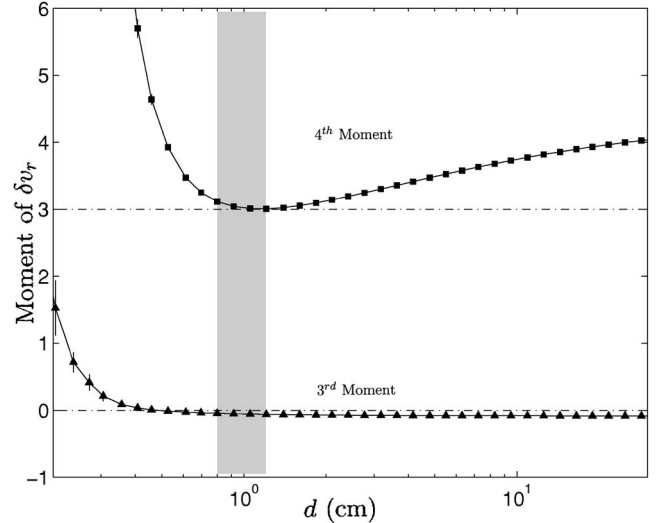

FIG. 4. The dependence of the third and fourth moments of $P(\delta v_r)$ on the size d of the subsystems. For sufficiently small d, $P(\delta v_r)$ should be Gaussian, which means the values of the third and fourth moments should have the values zero and three, respectively. We find that at $d \approx 0.9$ cm, the conditional distribution Eq. (11) is close to Gaussian (see text).

III. EXPERIMENT

We describe here an experiment on turbulent Couette-Taylor flow by Lewis and Swinney [16,51], and in the next section we will analyze data from this experiment to deduce $P(\beta)$ and a prediction for $P(\delta v_r)$. The fluid was contained in the annular region between two concentric cylinders with an inner radius of $b = 22.085$ cm and an outer radius of $a = 15.999$ cm; thus the ratio of inner to outer radius was 0.724. The height of the annulus was 69.5 cm, which yields a value of 11.4 for the ratio of height to the gap. The inner cylinder angular rotation rate Ω was $8 \times 2\pi$ rad/s; the outer cylinder was at rest. The ends of the annulus rotated at the same rate as the inner cylinder. The fluid was water with a viscosity ν of 0.00968 cm^2/s at the working effective temperature. Defining the Reynolds number as Re$=\Omega a(b-a)/\nu$ yields for the Reynolds number 540 000 [16].

A hot film probe was used to measure the time dependence of the azimuthal component of the velocity in the center of the gap at a distance 4.35 cm above midheight of the annulus. The Taylor frozen turbulence hypothesis was used to convert the velocity time series data to velocity field data. The turbulent intensity (the ratio of the root mean squared velocity to the mean velocity) was <6%.

The uncertainties shown on our graphs correspond to the standard deviation of 20 independent experiments. The velocity measurements were made with a sampling rate 2500 times the inner cylinder rotation frequency; this corresponds to a spatial separation of 0.017 cm between successive velocity values. The longitudinal velocity differences δv_r that we analyze are for points separated by a small distance, $r = 0.134$ cm, where the probability distribution function has approximately exponential tails [16]. An example of the measurements of $\delta v_r(t)$ is shown in Fig. 1. The separation $r = 0.134$ cm corresponds to 46η, where η is the Kolmogorov

scale [16]. (The Kolmogorov dissipation scale was obtained by calculating the dissipation from energy spectra: $\eta \equiv (\nu/\varepsilon)^{1/4}$, where the dissipation rate is given by $\varepsilon = 15\nu \int k^2 E(k) dk$ [16].) The window size d we use for determining the local inverse effective temperature β is typically 0.9 cm, nearly an order of magnitude larger than the value of r.

IV. RESULTS

A. Probability density function of inverse effective temperature

Several distributions for inverse effective temperature β_d have been discussed by Beck and Cohen [15]. Here we consider the log normal and χ^2 distributions, which are most applicable to turbulent flow. Due to multiplicative processes in turbulence, the log-normal distribution is often observed for positive-definite quantities (such as ε_r) [14,17–21]. A lognormally distributed β_d is given by

$$P(\beta_d) = \frac{1}{s(2\pi)^{1/2}\beta_d} \exp\left(-\frac{(\log\beta_d - m)^2}{2s^2}\right) \quad (11)$$

where $s = \sqrt{\ln(1 + \sigma_{\beta_d}^2/\bar{\beta}_d^2)}$ and $m = \log(\bar{\beta}_d^2/\sqrt{\bar{\beta}_d^2 + \sigma_{\beta_d}^2})$ are parameters, and $\bar{\beta}_d$ and σ_{β_d} are respectively the mean and standard deviation of β_d.

The χ^2 distribution of β_d is given by

$$P(\beta_d) = \frac{1}{\beta_d \Gamma(c)} \left(\frac{\beta_d}{b}\right)^c \exp\left(-\frac{\beta_d}{b}\right) \quad (12)$$

where $c = \bar{\beta}_d^2/\sigma_{\beta_d}^2$ and $b = \sigma_{\beta_d}^2/\bar{\beta}_d$ and Γ is the gamma function. The χ^2 distribution has been observed in recent measurement of wind turbulence [52]. The statistical properties

of different distributions are discussed in [15].

The experimental PDF for β_d is compared in Fig. 2 with a log-normal distribution and with a χ^2 distribution for two subsystem sizes d, 0.9 cm and 3 cm. The mean $\bar{\beta}_d$ and variance $\sigma^2_{\beta_d}$ of the inverse effective temperature determine the parameters s, m, b, and c. For small d, the log-normal and χ^2 differ significantly, but for large d they become closer together [Figs. 2(c) and 2(d)]. The decrease in variance of β_d with increasing d is similar to decrease observed in the variance of ϵ_r with increasing r [53].

The difference between the PDF of β_d from experiment and the χ^2 and log-normal distributions is shown in Figs. 2(b) and 2(d). For $d = 0.9$ cm, the log-normal distribution fits the data within the experimental uncertainty except small β_d regions, while the χ^2 distribution deviates from the observations by an amount that is large compared to the uncertainty. For $d = 3$ cm, the log-normal distribution fits the distribution of β_d, whereas the χ^2 distribution does not.

The log normal distribution (11) involves two parameters, s and m, which depend on subsystem size, as shown in Fig. 3. This figure suggests a relationship between s and m, $m = s^2/2$, which is supported by a calculation in Castaing *et al.* (see Sec. 4.3.1 in [14]).

B. Conditional probability and the proper subsystem size

In the statistical approach of Beck and Cohen, the subsystem size d should be sufficiently small so that $P(\beta_d)$ is Gaussian, corresponding to local thermodynamic equilibrium in the subsystems. However, in practice the $d \to 0$ limit is inaccessible because as d becomes very small, the number of data points becomes too small to allow accurate determination of the variance of β_d. So what is optimal choice of d? We address this question by examining the third moment (skewness) and fourth moment (kurtosis) of δv_r, which should be equal respectively to zero and three for a Gaussian distribution. In principle we could also examine fifth and higher moments, but because of the sensitivity of the higher moments to noise, we limit our considerations to the third and fourth moments. Plotting the third and fourth moments as a function of d, as shown in Fig. 4, we find that the optimal value of d for our data is 1.0–1.2 cm, which is the only range in which the kurtosis is approximately given by the value for a Gaussian. The skewness is small and negative for $d > 0.5$ cm, but becomes strongly positive for $d < 0.5$ cm, reflecting a cascade of energy to smaller length scales. We conclude that $d = 0.9$ cm is the optimal subsystem size for our data.

C. Probability distribution of δv_r

We found a log-normal distribution of β_d fits the turbulence data over a wide range in d (Sec. IV A). With the log normal distribution of β_d for the optimal value of d (0.9 cm, Fig. 4) and the conditional Gaussian distribution of δv_r for that β_d, we obtain the probability distribution of δv_r by the method of Beck and Cohen,
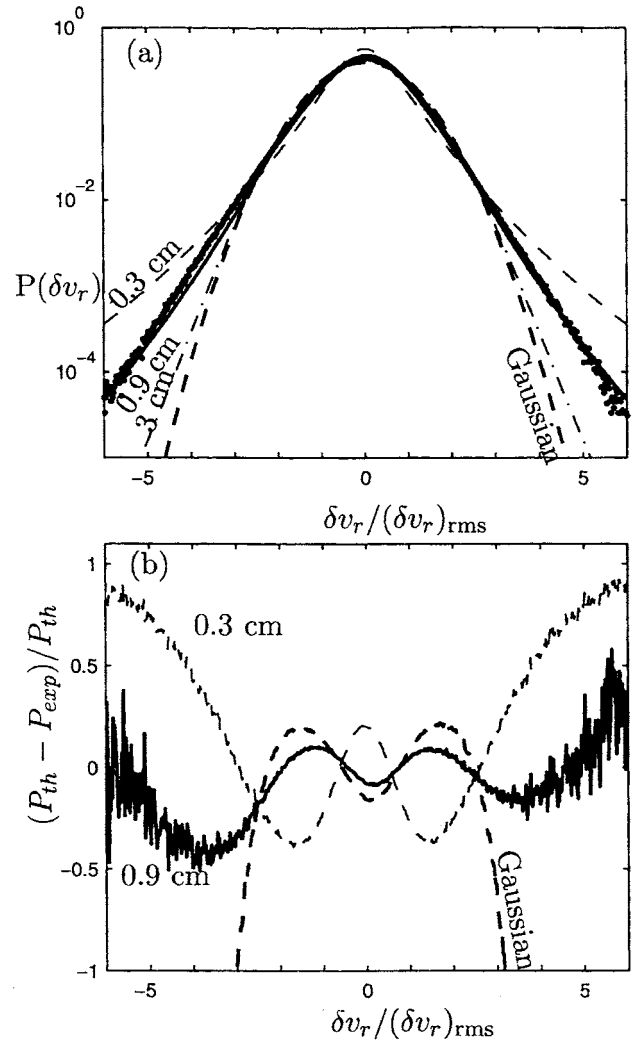

FIG. 5. Comparison experimental results (dots) for $P(\delta v_r)$ with the prediction of the Beck-Cohen method for a subsystem with the optimal size of 0.9 cm (bold line) on a semilog scale in (a) and relative error between theoretical and experimental values in (b). For comparison, we also show in (a) and (b) the predictions for subsystems of size 0.3 cm (thin dashed line) and 3 cm (thin dashed-dotted line), and a Gaussian distribution (dashed line).

$$P(\delta v_r) = \frac{1}{2\pi s} \int_0^\infty d\beta_d \beta_d^{-1/2} \exp\left(-\frac{(\log \beta_d - m)^2}{2s^2}\right)$$
$$\times \exp\left(-\frac{1}{2}\beta_d(\delta v_r)^2\right), \tag{13}$$

where s and m are determined from experiment for the optimal subsystem size d. There is no explicit form for the improper integral in Eq. (13) so we evaluate the integral numerically, using the limits ([$\min \beta_d, \max \beta_d$]) measured in experiments instead of the theoretical integral domain, [$0, \infty$).

The results for $P(\delta v_r)$ obtained by numerical integration of (13) are shown in Fig. 5. The data are described much better by the predicted probability distribution than by a Gaussian. The observed approximate power law tails are similar to the predicted distribution function.
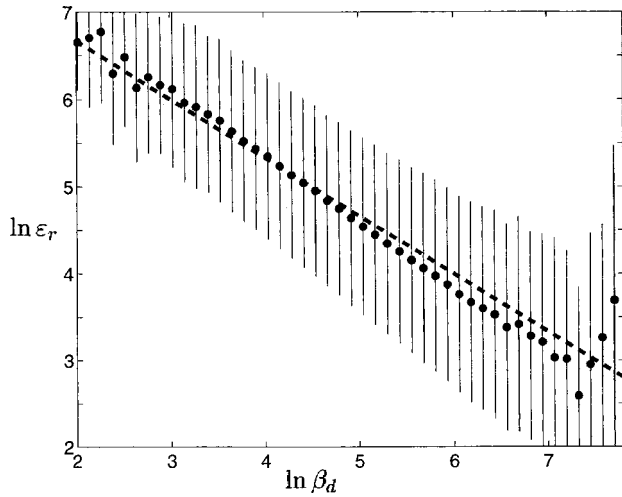
FIG. 6. The relation between β_d and ε_r. The solid vertical lines represent standard deviations at a fixed β_d and the dots represent the mean values. The dashed line is $\beta_d \propto (\varepsilon_r)^{-2/3}$.

D. Castaing and Beck-Cohen methods

If the two conditioning quantities in the Castaing and Beck-Cohen methods (ε_r and β_d, respectively) are correlated as a power-law, through Bayes' theorem the two methods can be seen to be the same [see Eq. (8)]. With the surrogate definition of ε_r as in Eq. (4) and a proper subsystem size (Sec. IV B), we find that β_d and ε_r exhibit a power-law relation, as Fig. 6 illustrates. In this sense, the Castaing and Beck-Cohen methods describe the same PDF of δv_r through the different conditional values which are correlated. Our experimental observation of a relation $\beta_d \propto (\varepsilon_r)^{-2/3}$ in Fig. 6 follows also from a dimensional analysis,

$$[\beta_d] = \left[\frac{T^2}{L^2}\right] = [L]^{-2/3} \times \left[\frac{L^2}{T^3}\right]^{-2/3} \Rightarrow \beta_d \propto r^{-2/3}\varepsilon_r^{-2/3},$$

(14)

where square brackets $[\cdot]$ denote the dimension of a physical quantity, T is the dimension of time and L is the dimension of length.

The probability of β_d conditioned to ε_r, $P(\beta_d|\varepsilon_r)$, is log-normally distributed, as Fig. 7 illustrates. Our assumption in Eq. (9) holds with the surrogate ε_r and β_d, where d is properly chosen (Sec. IV B). Thus the integral of two log-normal distributions, $\int P(\beta_d|\varepsilon_r)P(\varepsilon_r)d\varepsilon_r$, is another log-normal distribution, $P(\beta_d)$. That is, if $P(\beta_d|\varepsilon_r)$ is a log-normal distribution with the mean of $\ln \varepsilon_r$, a log-normal distribution of ε_r in Castaing's method is equivalent with a log-normal distribution of β_d in Beck-Cohen's method.

V. CONCLUSIONS

Both Castaing and Beck-Cohen methods have been very successful in describing the non-Gaussian distribution of velocity differences in turbulence [14,50]. Although the relation of Beck-Cohen's method and Tsallis statistics [61] to turbulence has been questioned [50,54–56], the fit to data is
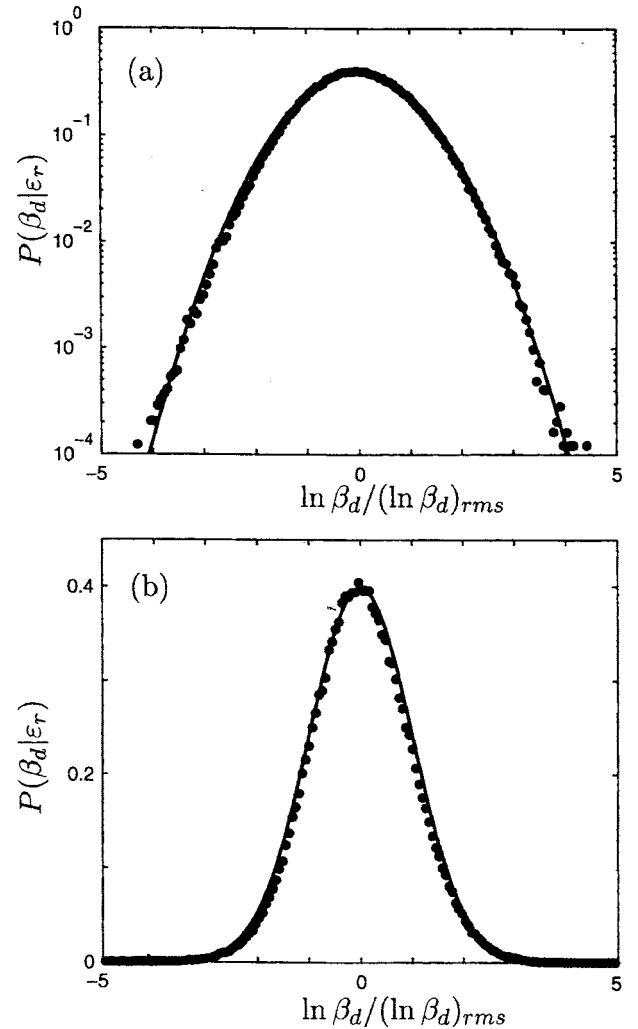

FIG. 7. The Gaussian distribution of $\ln \beta_d$ conditioned by ε_r, plotted on (a) log and (b) linear scales. The solid lines represent a Gaussian distribution of $\ln \beta_d$, that is, the log-normal distribution of β_d. The dots represent the mean values of $\ln \beta_d$ from experiments.

quite good [57–60]. We have presented a method for determining subsystem size in the Beck-Cohen method, thus eliminating the need for a fitting parameter.

We have also shown that Castaing's method can be converted to Beck-Cohen method—the log-normal distribution of ε_r in Castaing's method gives rise to a log-normal distribution of β_d in Beck-Cohen's method. In that sense, the two methods describe the non-Gaussian distribution of δv_r in the same way, $P(\delta v_r) = \int (\text{Gaussian distribution}) \times (\text{log-normal distribution})$.

[1] A. Kolmogorov, Dokl. Akad. Nauk SSSR **30**, 299 (1941).

[2] U. Frisch, *Turbulence, The Legacy of A.N. Kolmogorov* (Cambridge University Press, Cambridge, 1995).

[3] C. Van Atta and W. Chen, J. Fluid Mech. **44**, 145 (1970).

[4] E. Lifshitz and L. Landau, *Fluid Mechanics*, 2nd ed. (Butterworth-Heinemann, London, 1987), the remark on the variation of energy dissipation appeared in the 1st ed. in 1944.

[5] G. Batchelor and A. Townsend, Proc. R. Soc. London, Ser. A **199**, 238 (1949).

[6] H. Grant, R. Stewart, and A. Moilliet, J. Fluid Mech. **12**, 241 (1962).

[7] H. Grant, R. Stewart, and A. Moilliet, J. Fluid Mech. **224**, 429 (1991).

[8] A. Kolmogorov, J. Fluid Mech. **13**, 82 (1962).

[9] A. Obukhov, J. Fluid Mech. **13**, 77 (1962).

[10] G. Pedrizzetti, E. A. Novikov, and A. Praskovsky, Phys. Rev. E **53**, 475 (1996).

[11] H. Fujisaka, Y. Nakayama, T. Watanabe, and S. Grossmann, Phys. Rev. E **65**, 046307 (2002).

[12] S. Chen, K. Sreenivasan, and M. Nelkin, Phys. Rev. Lett. **79**, 1253 (1997).

[13] T. Nakano, D. Fukayama, A. Bershadskii, and T. Gotoh, J. Phys. Soc. Jpn. **71**, 2148 (2002).

[14] B. Castaing, Y. Gagne, and E. Hopfinger, Physica D **46**, 177 (1990).

[15] C. Beck and E. Cohen, Physica A **322**, 267 (2003).

[16] G. S. Lewis and H. L. Swinney, Phys. Rev. E **59**, 5457 (1999).

[17] B. Castaing, Y. Gagne, and M. Marchand, Physica D **68**, 387 (1993).

[18] A. Arneodo, S. Manneville, and J. Muzy, Eur. Phys. J. B **1**, 129 (1998).

[19] B. Castaing, Physica D **73**, 31 (1994).

[20] B. Chabaud, A. Naert, J. Peinke, F. Chilla, B. Castaing, and B. Hebral, Phys. Rev. Lett. **73**, 3227 (1994).

[21] B. Castaing and B. Dubrulle, J. Phys. II **5**, 895 (1995).

[22] A. Arneodo, J. Muzy, and S. Roux, J. Phys. II **7**, 363 (1997).

[23] P. Chainais, P. Abry, and J. Pinton, Phys. Fluids **11**, 3524 (1999).

[24] H. Kahalerras, Y. Malecot, Y. Gagne, and B. Castaing, Phys. Fluids **10**, 910 (1998).

[25] A. Arneodo, N. Decoster, and S. G. Roux, Phys. Rev. Lett. **83**, 1255 (1999).

[26] J. Pinton, F. Plaza, L. Danaila, P. Le Gal, and F. Anselmet, Physica D **122**, 187 (1998).

[27] L. Sorriso-Valvo, V. Carbone, P. Veltri, G. Consolini, and R. Bruno, Geophys. Res. Lett. **26**, 1801 (1999).

[28] P. Kailasnath, K. R. Sreenivasan, and G. Stolovitzky, Phys. Rev. Lett. **68**, 2766 (1992).

[29] P. Tabeling, G. Zocchi, F. Belin, J. Maurer, and H. Willaime, Phys. Rev. E **53**, 1613 (1996).

[30] P. Belin, F. Tabeling, and H. Willaime, Physica D **93**, 52 (1996).

[31] E. S. C. Ching and K. L. Chau, Phys. Rev. E **63**, 047303 (2001).

[32] Y. Gagne, M. Marchand, and B. Castaing, J. Phys. II **4**, 1 (1994).

[33] G. Stolovitzky, P. Kailasnath, and K. R. Sreenivasan, Phys. Rev. Lett. **69**, 1178 (1992).

[34] L. Wang, S. Chen, J. Brasseur, and J. Wyngaard, J. Fluid Mech. **309**, 113 (1996).

[35] R. Stewart, J. Wilson, and R. Burling, J. Fluid Mech. **41**, 141 (1970).

[36] M. Fisher and P. O. A. L. Davies, J. Fluid Mech. **18**, 97 (1964).

[37] O. Chanal, B. Chabaud, B. Castaing, and B. Hebral, Eur. Phys. J. B **17**, 309 (2000).

[38] J. Elsner and W. Elsner, Meas. Sci. Technol. **7**, 1334 (1996).

[39] J. C. Wyngaard and H. Tennekes, Phys. Fluids **13**, 1962 (1970).

[40] J.-F. Pinton and R. Labbé, J. Phys. II **4**, 1461 (1994).

[41] J. Wyngaard and S. Clifford, J. Atmos. Sci. **34**, 922 (1977).

[42] R. Antonia, N. Phan-Yhien, and A. Chambers, J. Fluid Mech. **100**, 193 (1980).

[43] J. Lumley, Phys. Fluids **8**, 1056 (1965).

[44] F. Champagne, J. Fluid Mech. **86**, 67 (1978).

[45] M. Nelkin, Adv. Phys. **43**, 143 (1994).

[46] C. Tsallis, J. Stat. Phys. **52**, 479 (1988).

[47] S. Gille and S. Smith, J. Phys. Oceanogr. **30**, 125 (2000).

[48] Stefan G. Llewellyn Smith and S. T. Gille, Phys. Rev. Lett. **81**, 5249 (1998).

[49] C. Beck, Europhys. Lett. **64**, 151 (2003).

[50] C. Beck, Physica D **193**, 195 (2004).

[51] D. P. Lathrop, J. Fineberg, and H. L. Swinney, Phys. Rev. A **46**, 6390 (1992).

[52] S. Rizzo and A. Rapisarda, in *Experimental Chaos: 8th Experimental Chaos Conference*, edited by S. e. a. Boccaletti (AIP, Florence, Italy, 2004), pp. 176–181.

[53] A. Turiel, G. Mato, N. Parga, and J. P. Nadal, Phys. Rev. Lett. **80**, 1098 (1998).

[54] T. Gotoh and R. H. Kraichnan, Physica D **193**, 231 (2004).

[55] M. Nauenberg, Phys. Rev. E **67**, 036114 (2003).

[56] C. Tsallis, Physica D **193**, 3 (2004).

[57] S. Jung, B. Storey, J. Aubert, and H. Swinney, Physica D **193**, 252 (2004).

[58] K. E. Daniels, C. Beck, and E. Bodenschatz, Physica D **193**, 208 (2004).

[59] N. Mordant, A. M. Crawford, and E. Bodenschatz, Physica D **193**, 245 (2004).

[60] C. Baroud and H. Swinney, Physica D **183**, 21 (2003).

[61] Beck and Cohen have shown that their method includes Tsallis statistics and other statistics [15]. A log-normal distribution is indistinguishable from Tsallis statistics except in long tails [50].